Radiology

Imaging Neoadjuvant Therapy Response in Breast Cancer[1]

Amy M. Fowler, MD, PhD
David A. Mankoff, MD, PhD
Bonnie N. Joe, MD, PhD

Online SA-CME
See www.rsna.org/education/search/ry

Learning Objectives:

After reading the article and taking the test, the reader will be able to:

- Identify indications for the use of neoadjuvant therapy in breast cancer.
- Compare the diagnostic accuracy of conventional breast imaging modalities in primary tumor therapy response assessment.
- Identify the strengths and limitations of functional and quantitative imaging techniques for assessing neoadjuvant therapy response in breast cancer.
- Categorize breast tumor response after neoadjuvant therapy by using MR imaging and fluorine 18 fluorodeoxyglucose PET-CT imaging

Accreditation and Designation Statement

The RSNA is accredited by the Accreditation Council for Continuing Medical Education (ACCME) to provide continuing medical education for physicians. The RSNA designates this journal-based SA-CME activity for a maximum of 1.0 *AMA PRA Category 1 Credit™*. Physicians should claim only the credit commensurate with the extent of their participation in the activity.

Disclosure Statement

The ACCME requires that the RSNA, as an accredited provider of CME, obtain signed disclosure statements from the authors, editors, and reviewers for this activity. For this journal-based CME activity, author disclosures are listed at the end of this article.

[1] From the Department of Radiology, University of Wisconsin School of Medicine and Public Health, 600 Highland Ave, Madison, WI 53792-3252 (A.M.F.); Department of Radiology, Perelman School of Medicine, University of Pennsylvania, Philadelphia, Pa (D.A.M.); and Department of Radiology and Biomedical Imaging, University of California–San Francisco School of Medicine, San Francisco, Calif (B.N.J.). Received January 24, 2017; revision requested March 13; final revision received June 13; accepted June 28; final version accepted July 12. **Address correspondence to** A.M.F. (e-mail: *afowler@uwhealth.org*).

Supported by School of Medicine and Public Health, University of Wisconsin-Madison (4KL2TR000428-10, 5KL2TR000428-09).

The use of neoadjuvant systemic therapy in the treatment of breast cancer patients is increasing beyond the scope of locally advanced disease. Imaging provides important information in assessing response to therapy as a complement to conventional tumor measurements via physical examination. The purpose of this article is to discuss the advantages and limitations of current assessment methods, as well as review functional and molecular imaging approaches being investigated as emerging techniques for evaluating neoadjuvant therapy response for patients with primary breast cancer.

Breast cancer mortality has declined since 1990 and this can be attributed to early detection through screening mammography and improved therapy (1). Local-regional therapies include surgery and radiation therapy. Adjuvant systemic therapies, including chemotherapy and/or endocrine therapy, are administered after surgery to eradicate potential micrometastatic disease. Adjuvant therapies have been shown to reduce the rates of disease recurrence and mortality for breast cancer patients (2,3).

Systemic therapy can also be administered before surgery, termed neoadjuvant or preoperative therapy. This has traditionally been used for locally advanced (clinical stage T3N1-N3M0) and inflammatory breast cancer (T4dN0-N3M0). However, neoadjuvant therapy is now being used in earlier stage breast cancer. The National Surgical Adjuvant Breast and Bowel Project B-18 and B-27 clinical trials compared disease-free and overall survival for patients with operable breast cancer at diagnosis randomized to either neoadjuvant or adjuvant chemotherapy and found no significant difference (4). Thus, patients who meet indications for adjuvant chemotherapy can be effectively treated in the neoadjuvant setting (5,6).

There are several benefits of neoadjuvant therapy. If the tumor is responsive, reducing its size before surgery could potentially convert an inoperable breast cancer to a resectable one or convert from complete mastectomy to partial mastectomy and/or lumpectomy (4,7). Another potential benefit of neoadjuvant therapy is that the extent of axillary surgery could be reduced. Pathologic response of the primary breast tumor correlates with axillary nodal response (8). There is growing evidence indicating that full axillary nodal dissection may be omitted for patients presenting with biopsy-proven node-positive disease that converts to clinically node-negative disease after neoadjuvant chemotherapy (8). Another important advantage is the ability to directly observe therapeutic efficacy when systemic therapy is given in the neoadjuvant setting; whereas there is no measurable disease to follow when therapy is given after surgery. This observation has led to the use of neoadjuvant therapy in clinical trials as a platform for accelerated approval of new drugs by the U.S. Food and Drug Administration (9).

Tumor response to neoadjuvant therapy can also provide prognostic information. The attainment of pathologic complete response (pCR) after completion of neoadjuvant therapy and surgical resection is associated with improved disease-free survival (10–12). This correlation is somewhat dependent on the molecular subtype and is strongest for patients with triple-negative (estrogen receptor [ER]-negative, progesterone receptor [PR]-negative, human epidermal growth factor receptor 2 [HER2]-nonamplified) and HER2-positive breast cancer (10–12).

Houssami et al (13) report the meta-analysis of more than 11 000 patients and provide evidence that there is an independent association between molecular subtype and pCR. For patients with triple-negative breast cancer, chemotherapy is the standard of care and has been shown to achieve a pCR rate of approximately 31% (13). For patients with HER2-positive disease, neoadjuvant chemotherapy is combined with HER2-targeted therapies with a pCR rate of 39% (13,14). These two patient populations have the best rates of pCR compared with the overall 19% pCR rate for all patients (13). As new targeted therapies continue to be developed for specific molecular subtypes, pCR rates are expected to increase. For example, more recent studies have shown pCR rates up to 60% with new HER2-targeted agents such as pertuzumab and trastuzumab-derivative of maytansine 1 (T-DM1) (15).

Essentials

- Prior to initiation of neoadjuvant therapy, diagnostic imaging should be performed for both breasts with additional whole-body imaging depending on the disease stage.
- The same imaging modality and protocol should be performed after completion of therapy for measurement of response together with repeat diagnostic mammography and/or US for preoperative localization planning if breast-conserving surgery is planned.
- Dynamic contrast-enhanced MR imaging of the breast offers the highest diagnostic accuracy in primary tumor therapy response assessment among the currently established methods (physical examination, mammography, and US).
- Functional and molecular imaging, using advanced MR imaging techniques and/or radionuclide imaging, are emerging methods for assessing physiologic changes induced by treatment and may indicate response earlier than anatomic-based imaging.
- Prospective, response-guided clinical trials are needed to demonstrate that use of functional and molecular imaging to guide neoadjuvant therapy management improves patient outcomes before widespread clinical adoption can occur.

https://doi.org/10.1148/radiol.2017170180

Content code: BR

Radiology 2017; 285:358–375

Abbreviations:

ACRIN = American College of Radiology Imaging Network
ADC = apparent diffusion coefficient
DCE = dynamic contrast material enhanced
ER = estrogen receptor
FDG = fluorine 18 fluorodeoxyglucose
FLT = fluorine 18 fluorothymidine
HER2 = human epidermal growth factor receptor 2
K^{trans} = volume transfer constant
NCCN = National Comprehensive Cancer Network
pCR = pathologic complete response
PR = progesterone receptor
SUV = standardized uptake value
tCho = total choline-containing compound

Conflicts of interest are listed at the end of this article.

Patients with hormone-receptor–positive breast cancer have the lowest pCR rate in response to neoadjuvant chemotherapy at 8% (13). Thus for patients with strongly positive hormone-receptor expression (ER positive and/or PR positive), neoadjuvant endocrine therapy can be considered. While most clinical trials of neoadjuvant endocrine therapy utilize treatment durations of 3–4 months, maximal response may require more time (16,17). Given the long duration and limited pCR rates, neoadjuvant therapy for patients with well-differentiated ER-positive disease is not used frequently.

Studies of neoadjuvant therapy have used a variety of methods for assessing tumor response. Currently, there are no established clinical practice guidelines for how best to assess tumor response to neoadjuvant therapy. Typically, patients undergo conventional breast imaging (mammography and ultrasonography [US]) and physical examination. The purpose of this article is to discuss the advantages and limitations of current assessment methods, as well as review functional and molecular imaging modalities being investigated as emerging techniques for evaluating neoadjuvant therapy response for patients with localized, nonmetastatic primary breast cancer.

Current Methods

Current methods for evaluating tumor response to neoadjuvant therapy consist of physical examination and conventional breast imaging with mammography and US (Figs 1, 2). Physical measurement of tumor size with calipers is typically performed prior to each chemotherapy cycle or monthly if neoadjuvant endocrine therapy is used (18). The accuracy of clinical breast examination for determining pCR in patients with locally advanced breast cancer after neoadjuvant hormonal or chemotherapy is 57%, which is inferior to mammography (74%) and US (79%) (19). Challenges with physical examination include the presence of firm fibroglandular tissue and posttherapy fibrosis, which can overestimate the amount

Figure 1

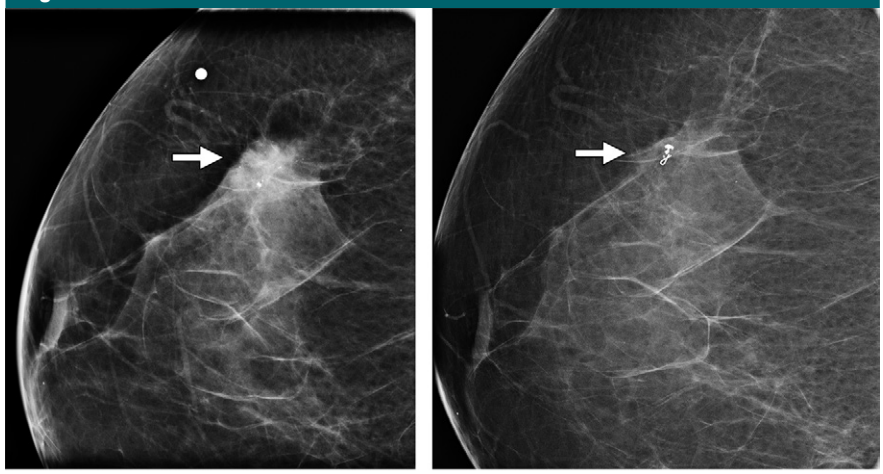

a. b.

Figure 1: Images of a 65-year-old woman with a palpable mass in the right breast. **(a)** Spot compression craniocaudal diagnostic mammogram shows a 1.8-cm irregular high-density mass with indistinct margins and associated microcalcifications (arrow). Biopsy results demonstrated grade 3, ER-positive, PR-positive, HER2-negative invasive lobular carcinoma. **(b)** Diagnostic mammogram following neoadjuvant therapy shows resolution of the mass and a biopsy clip (arrow) adjacent to a coarse dystrophic calcification. Pathologic complete response was confirmed with lumpectomy.

Figure 2

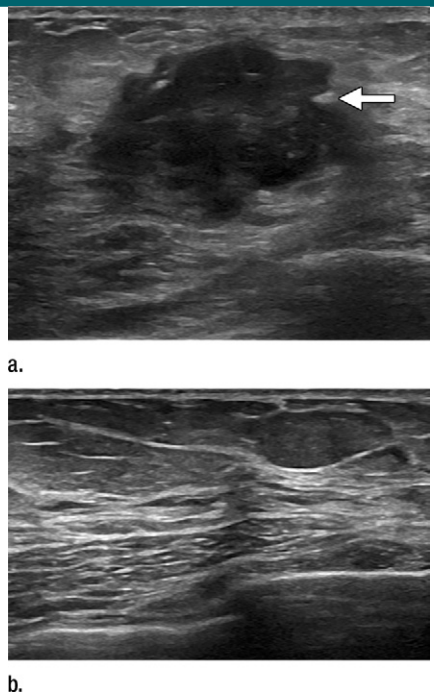

a.

b.

Figure 2: Images of a 65-year-old woman with a palpable mass in the left breast. **(a)** US scan after diagnostic mammography shows a corresponding 3.1-cm irregular hypoechoic mass with angular margins (arrow). Biopsy results demonstrated grade 3, ER-positive, PR-negative, HER2-amplified invasive ductal carcinoma. **(b)** US scan after neoadjuvant chemotherapy and HER2-directed therapy demonstrates minimal acoustic shadowing in the area of previously biopsied mass, indicated by the biopsy marker clip, consistent with imaging response to therapy. pCR was confirmed with lumpectomy.

Table 1

Current Breast Imaging Utilized Prior to Neoadjuvant Therapy

Variable	Mammography*	Breast US†	Breast MR Imaging‡
Ipsilateral breast	Extent of disease evaluation: full-field craniocaudal, full-field mediolateral oblique, full-field mediolateral/ lateromedial plus spot compression craniocaudal, spot compression mediolateral/ lateromedial	Extent of disease evaluation targeted to index lesion	Extent of disease evaluation: pectoralis/chest wall invasion
Contralateral breast	Screening: full-field craniocaudal, full-field mediolateral oblique	Not typically performed	Screening
Lymph nodes§	Lymphadenopathy evaluation: axillary (incomplete)	Lymphadenopathy evaluation: axillary	Lymphadenopathy evaluation: axillary, internal mammary

* Digital breast tomosynthesis may be utilized as part of the diagnostic evaluation. Substitute spot compression views with magnification craniocaudal and mediolateral/lateromedial views if associated microcalcifications.

† Whole-breast US may be performed for patients unable to undergo magnetic resonance (MR) imaging, particular for patients with mammographically dense breasts. However, the relatively high rate of false-positive findings limits recommendation of this approach.

‡ Utilization of breast MR imaging may vary with clinical practices due to surgeon and/or oncologist preferences.

§ Fluorine 18 fluorodeoxyglucose (FDG) positron emission tomography (PET)/computed tomography (CT) imaging may be helpful for evaluating regional nodal sites of disease (axilla, internal mammary, and supraclavicular) for locally advanced breast cancer, especially in patients presenting with more advanced axillary disease.

of residual disease. Likewise, interval loss of palpability after treatment does not exclude the presence of residual tumor.

Conventional breast imaging is performed prior to the start of neoadjuvant therapy (Table 1). Diagnostic mammography should include full-field craniocaudal, mediolateral oblique, and mediolateral views, with spot compression or magnification images at the site of malignancy and full-field craniocaudal and mediolateral oblique views of the contralateral breast. Digital breast tomosynthesis may be utilized as part of the diagnostic evaluation. Targeted US should be performed for malignant breast masses and of the axilla for clinical staging if neoadjuvant therapy is planned. The goals of pretherapy imaging are to determine the imaging extent of disease, for local-regional staging, and to screen the contralateral breast. Also, it is important to confirm appropriate biopsy marker clip placement within the breast tumor and axillary lymph node, if sampled, prior to the start of neoadjuvant therapy in case a complete imaging response is obtained.

Utilization of whole-body imaging for initial systemic staging is based on patient symptoms and clinical stage. National Comprehensive Cancer Network (NCCN) guidelines state that systemic imaging can be considered for patients with clinical stage IIB with advanced axillary disease, stage III, locally advanced, and inflammatory breast cancer, particularly if signs or symptoms are present (20). Modalities include chest CT, CT or MR imaging of the abdomen and pelvis, bone scan or sodium fluoride PET/CT, and FDG PET/CT. For asymptomatic patients with early-stage breast cancer, routine systemic staging is not indicated. After completion of therapy, the same modality and protocol should be used to assess treatment response and to determine the amount of residual disease for surgical planning (lumpectomy vs mastectomy) and preoperative localization. NCCN guidelines recommend "physical examination and performance of imaging studies that were abnormal at the time of initial staging" (20). Recommendations include the optional use of breast MR imaging before and after neoadjuvant therapy, which may be helpful for mammographically occult tumors. Close communication with the multidisciplinary care team is encouraged for selection of the appropriate imaging prior to surgery.

Mammography and US

Data regarding the diagnostic accuracy of mammography and US for assessing response to neoadjuvant therapy are variable. In a report of six studies, the accuracies of mammography and US for determining postneoadjuvant pathologic tumor response were 74% and 79%, respectively (19). Mammography has been shown to be more sensitive than physical examination for detecting presence of residual tumor after therapy but is less specific and may underestimate the degree of treatment response (21,22). The mammographic lesion type, such as architectural distortion, and margin impact its accuracy for size measurement, with decreased accuracy when margins are indistinct or spiculated and due to masking from adjacent normal tissue (23). Use of digital breast tomosynthesis, which reduces the masking effect, may improve measurement accuracy (24). Additional challenges with mammography include the presence of microcalcifications, which do not correlate with presence of viable tumor (25–27).

US has been shown to be a better predictor for pathologic tumor size than mammography after treatment with neoadjuvant therapy (19,28,29). Furthermore, US is the most accurate predictor of response in axillary lymph nodes compared with mammography and physical examination (30). The best method for predicting complete pathologic response appears to be the

Figure 3

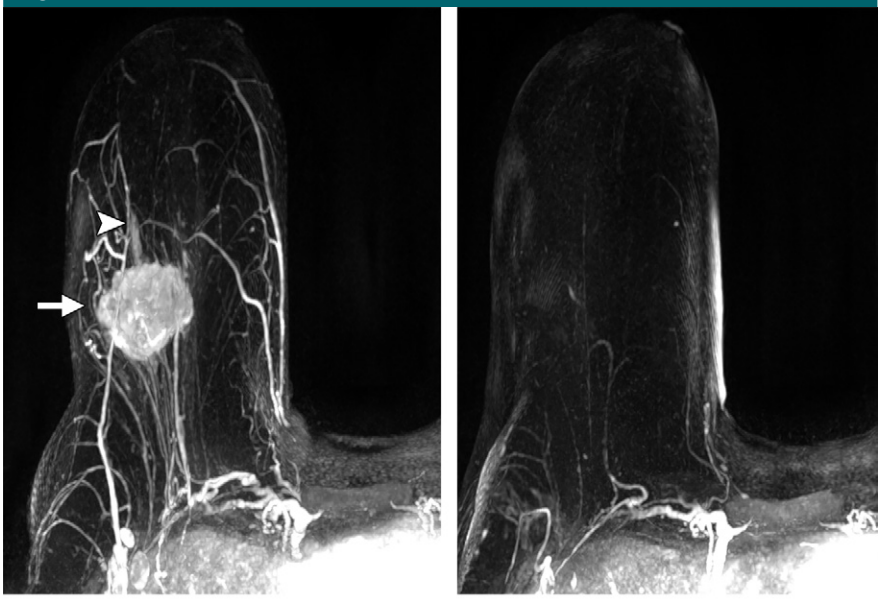

a. b.

Figure 3: Images of a 57-year-old woman with newly diagnosed clinical stage IIA (T2N0M0) right breast cancer. Histologic results were grade 3, ER-negative, PR-negative, HER2-nonamplified invasive ductal carcinoma with extensive necrosis. **(a)** Maximum intensity projection from contrast material–enhanced breast MR imaging performed prior to neoadjuvant chemotherapy demonstrates a 3.3-cm irregular right breast mass with rim enhancement (arrow) and 1.8 cm of linear nonmass enhancement extending anterior to the mass (arrowhead). **(b)** Breast MR images after neoadjuvant chemotherapy shows resolution of the abnormal enhancement. Final pathologic findings after breast-conserving surgery showed complete pathologic response. Images were obtained by using a 1.5-T unit with an eight-channel radiofrequency breast coil. Maximum intensity projection images are the subtraction of precontrast from first postcontrast axial three-dimensional fat-suppressed T1-weighted gradient-echo sequences (echo time msec/repetition time msec, 2.9/6.0; 10° flip angle).

combination of mammography with US (80% likelihood when findings of both modalities are negative) (29,31).

MR Imaging

Breast MR imaging is the most sensitive modality for breast cancer detection (32) and is the most accurate imaging modality for assessment of tumor response to neoadjuvant therapy (Figs 3, 4) (19,33–37). In a combined analysis of six studies, the positive predictive value (ability to correctly predict the presence of residual disease at final pathologic examination) was high at 93% (19). The negative predictive value (ability to correctly predict the absence of disease at final pathologic examination) was only moderate at 65%, which decreased the overall diagnostic accuracy to 84% (19). Additional diagnostic performance data from several meta-analyses are summarized in Table 2 (34–37). MR imaging has better accuracy compared with mammography, US, or clinical breast examination (19,38). Despite these promising data, MR imaging is not currently reliable enough to allow patients to avoid surgical resection after complete imaging response.

A prospective, multi-institutional trial that validated the accuracy of breast MR imaging for assessment of neoadjuvant therapy response is the American College of Radiology Imaging Network (ACRIN) 6657 study, which was performed in conjunction with the multi-institutional Investigation of Serial Studies to Predict Your Therapeutic Response with Imaging And molecular Analysis (I-SPY TRIAL) (38). This study involved 216 women with stage II or stage III breast cancer treated with neoadjuvant chemotherapy. The highest predictive value for predicting pathologic response after neoadjuvant chemotherapy was achieved by using both MR imaging and clinical measurements of tumor size (38). MR imaging tumor size estimates by using volume measurements were superior to measurements of the longest diameter for predicting therapy response (38). Furthermore, MR imaging functional tumor volume was shown to predict recurrence-free survival (39). Functional tumor volume is a computer-estimated tumor volume using the signal enhancement ratio method, a voxel-based quantitative technique comparing signal intensities on pre-, early, and late postcontrast images (38).

There is overall good agreement between residual tumor size measured on MR images and pathologic tumor size determined after surgical excision. Studies have shown that MR imaging can overestimate or underestimate residual tumor size, with a median correlation coefficient of 0.70 (range, 0.21–0.98) reported in a systematic review by Lobbes et al (33). The potential clinical impact of overestimation of residual tumor size is the resection of a larger amount of tissue during breast-conserving surgery, which may negatively alter cosmetic outcome or influence a decision for mastectomy. The impact of underestimation of residual tumor size is the potential for an incomplete resection with positive surgical resection margins and need for reoperation.

There are several factors that have been shown to affect the diagnostic accuracy of MR imaging for therapy response assessment. Tumor molecular subtype is one key factor. Accuracy of MR imaging in determining residual tumor size after neoadjuvant therapy is greatest in ER-negative/HER2-positive and triple-negative tumors and is less accurate in luminal tumors (40,41). The type of chemotherapy regimen can also influence diagnostic accuracy of MR imaging, which can underestimate residual disease in patients treated with taxanes and antiangiogenic drugs, through hypothesized antivascular effects on contrast enhancement (42,43). The pattern

of tumor response can also impact MR imaging accuracy. For instance, MR imaging can underestimate residual disease when fragmentation occurs and small foci of residual tumor cells are scattered over a large area or overestimate residual disease if there is host response of reactive inflammation and fibrosis within the treated tumor bed (42,44). Lastly, the use of pathologic response criteria that allow for the presence of noninvasive disease in their definition of complete response can negatively affect the accuracy of imaging response assessment since noninvasive disease may still be visualized with imaging.

Utilization of breast MR imaging for evaluation of response to neoadjuvant therapy is included as one of the recommended clinical indications by the American College of Radiology and European Society of Breast Imaging (45,46) and is included in the NCCN guidelines as an optional tool (20). Despite inclusion in several clinical practice guidelines, preoperative breast MR imaging is not universally utilized. There are two main limitations. Long-term patient survival outcomes are not yet known and it has been speculated that finding small additional tumors at MR imaging will be unlikely to alter mortality since they may be effectively treated with chemotherapy and/or radiation therapy. Furthermore, there is concern regarding the potential delay in definitive treatment caused by detection of false-positive lesions requiring additional US imaging and US or MR imaging-guided biopsy. Patient-specific factors such as inability to tolerate prone positioning, claustrophobia, pacemaker, pregnancy, and renal impairment are minor and infrequent limitations.

Figure 4

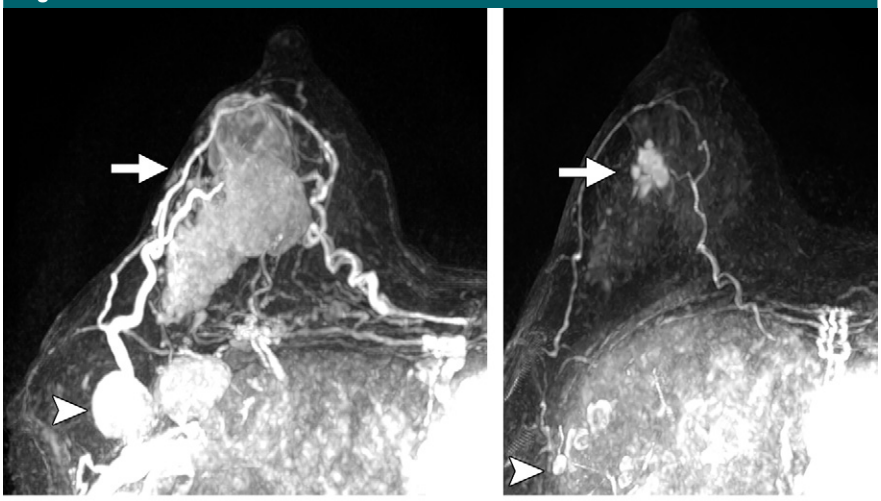

a. b.

Figure 4: Images of a 37-year-old woman with newly diagnosed clinical stage IIIA (T3N1M0) right breast cancer and metastatic axillary lymphadenopathy. Histologic results were grade 3, ER-negative, PR-negative, HER2-amplified invasive ductal carcinoma with ductal carcinoma in situ with Ki67 index of 70%. **(a)** Maximum intensity projection from contrast-enhanced breast MR imaging performed prior to neoadjuvant chemotherapy demonstrates a 6.4-cm enhancing right breast mass (arrow) and axillary lymphadenopathy (arrowhead). **(b)** Breast MR image after neoadjuvant chemotherapy shows partial response of the primary breast cancer (arrow) and decreased right axillary lymphadenopathy (arrowhead). Final pathologic findings after breast-conserving surgery showed residual stage IB disease (ypT1c ypN1mic). Images were obtained by using a 1.5-T unit with an eight-channel radiofrequency breast coil. Maximum intensity projection images are the subtraction of precontrast from first postcontrast axial three-dimensional fat-suppressed T1-weighted gradient-echo sequences (2.9/6.0, 10° flip angle).

Functional and Molecular Imaging

While conventional imaging (mammography, US, and contrast-enhanced MR imaging) and physical examination are the methods currently used clinically, a major drawback of these approaches is their reliance on changes in lesion size to measure tumor response. Systemic therapies require time to reach steady-state levels, induce cellular changes leading to cell death, and ultimately

Table 2

Meta-Analyses of Breast MR imaging for Evaluation of Neoadjuvant Therapy Response

Meta-Analysis	No. of Studies	No. of Patients	Pooled Sensitivity (%)	Pooled Specificity (%)	Likelihood Ratio Positive	Likelihood Ratio Negative	Diagnostic Odds Ratio
Yuan et al 2010 (34)	25	1212	63 (56–70)*	91 (89–92)*	Not reported	Not reported	17.05 (10.59–27.19)
Wu et al 2012 (35)	30	1496	68 (57–77)*	91 (87–94)*	7.48 (5.29–10.57)	0.36 (0.27–0.48)	20.98 (13.24–33.24)
Marinovich et al 2013 (36)	44	2050	83–87†	54–83†	Not reported	Not reported	Not reported
Sheikbahaei et al 2016 (37)	10	492	88 (76–95)	55 (41–68)	Not reported	Not reported	Not reported

Note.—Data in parentheses are the range.

* Sensitivity defined as ability to correctly identify patients achieving pCR after preoperative therapy. Specificity defined as ability to correctly identify nonpCR after preoperative therapy.

† Sensitivity defined as ability to correctly identify presence of residual tumor after preoperative therapy in patients with nonpCR. Specificity defined as ability to correctly identify absence of residual tumor after preoperative therapy in patients with pCR.

Table 3

Functional and Quantitative Imaging Techniques for Assessing Neoadjuvant Therapy Response in Breast Cancer

Technique	Biologic Parameter	Feasibility for Clinical Practice	Advantages	Challenges/Barriers
SER and pharmacokinetic DCE MR imaging	Tumor vascularity	Moderate for SER-based analyses; Pharmacokinetic analyses remain investigational	Demonstrated association with patient survival outcomes for certain SER-based parameters	Requires excellent image quality without motion artifact; difficult to standardize technique for pharmacokinetic analyses; requires additional postprocessing to obtain pharmacokinetic and SER parameters
Diffusion-weighted MR imaging	Tumor cellularity	Strong, in some current clinical practices	No intravenous contrast material requirement	Requires excellent imaging quality and fat suppression; image distortion problematic; no standardization for b-values; requires additional postprocessing to calculate ADC values for quantitative analysis
Proton MR spectroscopy	Choline metabolism	Possible, remains investigational	No intravenous contrast material requirement, but placement of spectroscopic volume of interest often based on contrast-enhanced images	Requires excellent magnetic field homogeneity; long acquisition time; limited coverage area for breast; difficult to perform successfully; difficult to standardize technique
FDG-PET	Glucose metabolism	Strong, in many current clinical practices	Readily available radiopharmaceutical	No census for timing and SUV cutoff; uptake in inflammation
FLT-PET	Tumor proliferation	Moderate, remains investigational but has undergone multicenter testing	Correlation with Ki67 biomarker for proliferation	No FDA approval for FLT; variable uptake among tumor subtypes
FACBC-PET	Amino acid metabolism	Possible, FDA-approved tracer used clinically for prostate cancer imaging	Strong uptake in invasive lobular carcinoma	Limited experience for breast cancer response evaluation
^{11}C-choline-PET	Choline metabolism	Possible, FDA-approved tracer used clinically for prostate cancer imaging	May indicate resistance to trastuzumab in HER2+ disease	Short half-life limits distribution; limited experience for breast cancer response evaluation

Note.—ADC = apparent diffusion coefficient, DCE = dynamic contrast enhanced, FDA = Food and Drug Administration, FACBC = anti-1-amino-3-^{18}F-fluorocyclobutane-1-carboxcylic acid, FLT = fluorine 18 fluorothymidine, SER = signal enhancement ratio, SUV = standardized uptake value.

decrease tumor size. A reliable method for early identification of tumors that are not responding would be helpful in directing these patients to definitive surgical treatment and avoid continual risk of side effects from ineffective therapy. Another potential benefit would be the ability to change therapy before going to surgery. However, the use of serial imaging to alter neoadjuvant therapy prior to definitive surgery is generally performed within adaptive or response-guided clinical trial settings (47,48). Quantitative, functional imaging such as advanced MR imaging techniques and radionuclide imaging (Table 3) may be useful for assessing physiologic changes for therapy response evaluation.

The functional and molecular imaging techniques discussed in the following sections are not routinely performed in clinical practice and are primarily investigational at this time. It is essential for successful clinical adoption that quantification can be performed easily and reproducibly across a variety of platforms and that incorporation of imaging data to guide treatment decisions can be shown to improve patient outcomes.

Pharmacokinetic Analysis of DCE Perfusion MR Imaging

DCE MR imaging consists of multiple sets of images acquired after injection of gadolinium-based contrast agents, which shorten the T_1 relaxation time and increase the signal intensity of tissue with increased microvessel density and permeability (49). Accumulation of contrast material observed within malignant lesions is related to tumor angiogenesis and disorganized, leaky microvasculature, which typically enhance rapidly initially followed by wash-out of contrast material (50). The amount of tissue signal enhancement is plotted over time, which can be fit to various pharmacokinetic models. Typically, a simple two-compartment mathematical model is used consisting of blood plasma and the extravascular extracellular space. Parameters derived from modeling reflect important physiologic parameters, such as tissue perfusion, microvessel wall permeability, microvessel density, and intravascular and extracellular extravascular volume fractions. Definitions for the most commonly used kinetic parameters were standardized by Tofts et al, which include *(a)* the volume transfer constant (K^{trans}) between the extravascular extracellular

space and plasma (in min^{-1}), *(b)* the volume of extravascular extracellular space per unit volume of tissue, or v_e, (unitless), and *(c)* the flux rate constant between the extravascular extracellular space and plasma, or k_{ep} (in min^{-1}) ($k_{ep} = K^{trans}/v_e$) (51). Other parameters include the vascular volume fraction, or v_p, (blood plasma volume per unit volume of tissue), the integrated area under the gadolinium curve, or IAUGC (in mmol $L^{-1}sec^{-1}$), and the mean transit time for contrast material to perfuse a region of interest (in seconds). While visual assessment of contrast enhancement and lesion morphology is the essential component of clinical breast MR imaging interpretation, pharmacokinetic analysis of contrast enhancement adds a quantitative aspect to the examination and reveals several biologic features including perfusion.

Effective chemotherapy reduces tumor neoangiogenesis and microvascular permeability, which occurs in part through the loss of proangiogenic growth factor support and altered endothelial cell function (52). Thus, changes in pharmacologic kinetic model parameters have been investigated in breast cancer patients undergoing neoadjuvant chemotherapy. An early study of whether changes in kinetic MR imaging parameters after one to two cycles of neoadjuvant chemotherapy can be used to predict pathologic response was published by Padhani et al (53). They found that K^{trans} values were reduced in patients achieving clinical-pathologic treatment response. Furthermore, both tumor size measured with MR imaging and K^{trans} were similarly accurate in predicting therapy nonresponsiveness after two treatment cycles. Additional studies have demonstrated that treatment response corresponds with decreases in K^{trans} and k_{ep}, while treatment nonresponse corresponds with increases in v_e, reviewed in reference 54. Two systematic reviews (55,56) have been published indicating that K^{trans} is a promising parameter for early identification of treatment response.

In addition to predicting pathologic response, changes in tumor perfusion during the course of neoadjuvant chemotherapy quantified by pharmacokinetic parameters may also predict patient outcome. Li et al (57) demonstrated higher recurrence rates and worse overall survival in a study of 62 patients with primary breast cancer undergoing neoadjuvant chemotherapy when high tumor vascularization (K^{trans}) was observed with DCE MR imaging after two cycles. Likewise, Woolf et al (58) showed that changes in the signal intensity-time curves of DCE MR imaging correlated with changes in K^{trans}, pathologic response, and overall survival in 73 primary breast cancer patients undergoing neoadjuvant chemotherapy.

Although clinical DCE breast MR imaging is routinely performed in accordance with American College of Radiology criteria, the use of DCE MR imaging for pharmacokinetic analysis is predominately investigational at this time. It has potential to be used clinically if quantification can be performed easily and reproducibly across a variety of vendor platforms. This has been identified as an important initiative by the Quantitative Imaging Biomarkers Alliance of the Radiological Society of North America, which provides consensus recommendations for standardized techniques and methodologic analyses of DCE MR imaging quantification (59).

Diffusion-weighted MR Imaging

Diffusion-weighted MR imaging is a quantitative imaging technique that may complement DCE MR imaging for evaluating tumor response to neoadjuvant therapy (Fig 5). Diffusion-weighted MR imaging is used to measure the random Brownian motion of water molecules within tissue and is quantified as an ADC. Tumor cellularity correlates with restricted diffusion of water molecules and thus inversely correlates with ADC (60,61). Most invasive breast cancers have lower ADC values (0.87 to 1.36 $\times$ 10^{-3} mm^2/sec) compared with normal tissue (1.51 to 2.09 $\times$ 10^{-3} mm^2/sec) (62). Reported cut-off points for distinguishing malignant from benign breast lesions vary from 0.90 to 1.76 $\times$ 10^{-3} mm^2/sec (62).

Cytotoxic chemotherapy damages cell membranes and reduces the number of viable malignant cells within a tumor, resulting in increased interstitial space and increased water diffusivity. ADC values increase after chemotherapy, with larger increases in pathologic responders compared with nonresponders (63,64). Changes in diffusion can be measured after only one cycle of chemotherapy and before tumor size changes can be measured by using morphologic criteria (65,66). A meta-analysis of the diagnostic accuracy of diffusion-weighted MR imaging (six studies; 294 patients) demonstrated summary sensitivity and specificity of 93% and 82%, respectively, for predicting response to neoadjuvant chemotherapy (35). This study also showed that diffusion-weighted MR imaging has high sensitivity while DCE MR imaging has high specificity for predicting pathologic response. A large multi-institutional clinical trial (ACRIN 6698) is ongoing, which aims to determine if changes in ADC values are predictive of pCR in patients treated with neoadjuvant chemotherapy in the I-SPY 2 TRIAL.

MR Spectroscopy

Another advanced quantitative imaging technique using MR imaging that is being investigated for therapy response assessment is hydrogen 1 (^1H) MR spectroscopy. While conventional MR imaging represents the total signal from all proton-containing molecules in a voxel of tissue, ^1H MR spectroscopy separates proton signals arising from fat, water, and other molecules such as lactate and choline-containing compounds, which are of interest in cancer tissue (67). The resonance peak of total choline-containing compounds (tCho), located at approximately 3.2 ppm, is elevated in malignant lesions compared with benign and normal breast tissue (68). It is hypothesized that the increased tCho peak observed in malignancies reflects increased cell membrane turnover and phosphocholine utilization and is an indirect indicator of cellular proliferation.

Studies have shown that the tCho resonance peak decreases or disappears completely in patients undergoing chemotherapy (69,70). Furthermore, these changes occur early in response

Figure 5

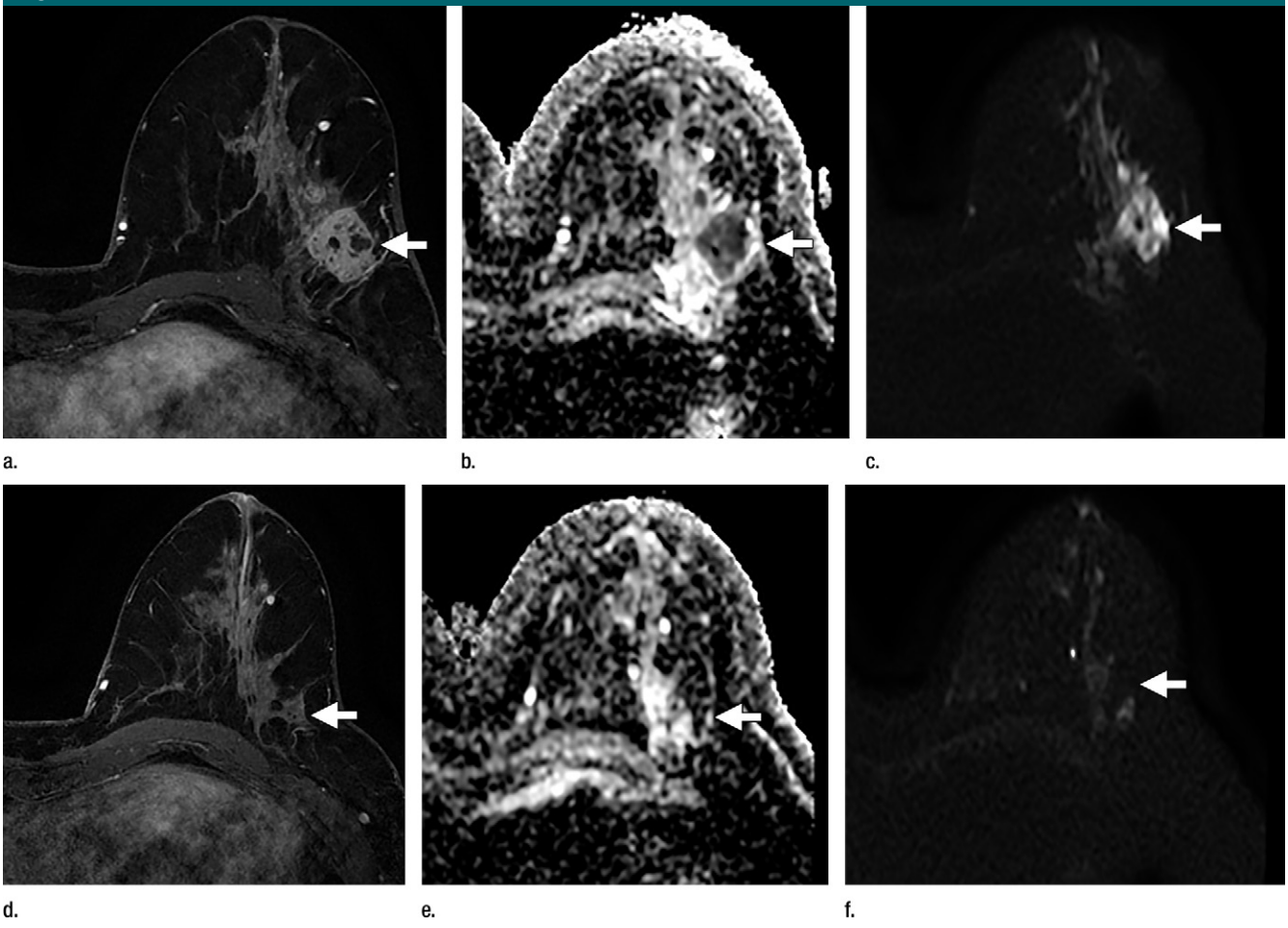

Figure 5: Images of a 65-year-old woman with newly diagnosed clinical stage IIB (T2N1M0) left breast cancer (breast US from same patient shown in Fig 2). Histologic findings demonstrated grade 3, ER-positive, PR-negative, HER2-amplified invasive ductal carcinoma. **(a–c)** Breast MR images prior to neoadjuvant chemotherapy with HER2-directed therapy demonstrate a 3.2-cm irregular enhancing mass (arrow) in the left breast on axial postcontrast (**a**) images with an ADC value of 0.63×10^{-3} mm^2/sec (**b**) and restricted diffusion (**c**). **(d–f)** Breast MR images during neoadjuvant chemotherapy demonstrate lack of residual enhancement (arrow) of the left breast mass (**d**), with normalization of the ADC (**e**) and diffusion signals (**f**) (arrow). Pathologic complete response was confirmed with lumpectomy. Images were obtained by using a 3.0-T unit with an eight-channel radiofrequency breast coil. First postcontrast images are from axial three-dimensional fat-suppressed T1-weighted gradient-echo sequences (2.5/5.2, 10° flip angle). Diffusion-weighted images are from axial two-dimensional spin-echo echo-planar imaging sequences (*b* value, 800 sec/mm^2; 74/4817; 90° flip angle).

to chemotherapy. Meisamy et al (71) demonstrated decreases in tCho within 24 hours of initial treatment, which were significantly different between responders and nonresponders, defined by the longest dimension in tumor size after completion of therapy. Baek et al (72) demonstrated reduction in tCho levels at the first imaging follow-up performed after one to two cycles of neoadjuvant chemotherapy in the group that responded with a decrease in tumor size but not in the nonresponding group.

Further investigation into the accuracy of using MR spectroscopy measurements of tCho levels for early therapy response prediction was performed through a large multi-institutional clinical trial (ACRIN 6657 MRS) (73). This study focused on early changes in tCho levels measured 1–4 days after starting chemotherapy. Unfortunately, technical challenges in acquiring quantitative MR spectroscopy data from the multiple sites were encountered, with only 29 of 119 subjects with analyzable data and eight with pCR. In the limited data set, early decreases in tCho after chemotherapy initiation had poor predictive ability for pCR or radiologic response. Current technical challenges associated with MR spectroscopy, such as operator variability in acquisition voxel placement and requirement of a 3-T system for improved signal-to-noise ratio, limit implementation into routine clinical practice (73,74). Thus, MR spectroscopy remains investigational at this time.

Figure 6

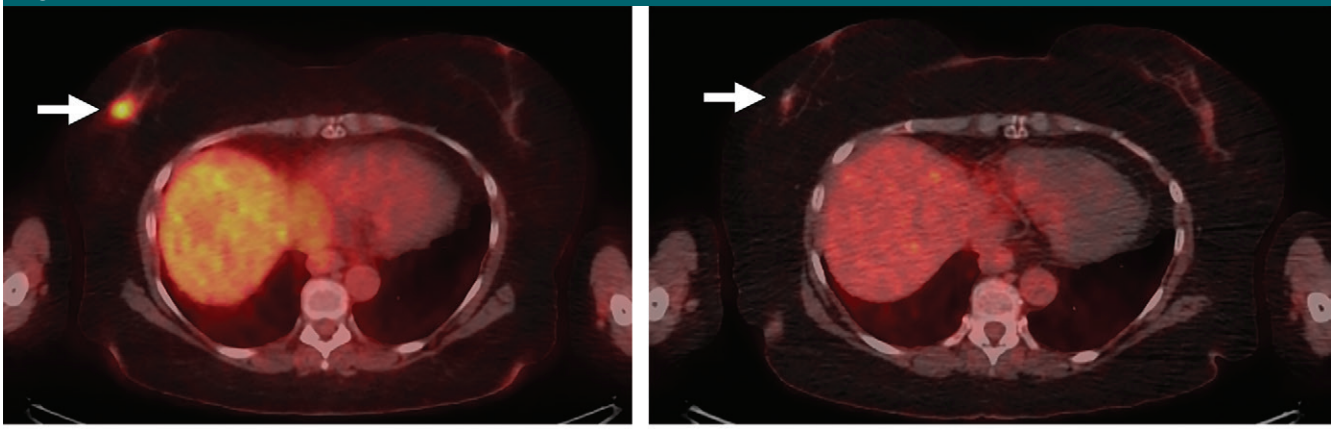

a. b.

Figure 6: Images of a 65-year-old woman with newly diagnosed right breast cancer and recurrent ovarian cancer (mammographic images from same patient shown in Fig 1). **(a)** Fused axial FDG PET/CT image demonstrates increased FDG uptake of the right breast mass (maximum SUV = 3.9) (arrow). Histologic results were grade 3, ER-positive, PR-positive, HER2-negative invasive lobular carcinoma. **(b)** Fused axial FDG PET/CT image following neoadjuvant chemotherapy and endocrine therapy with an aromatase inhibitor shows interval resolution of FDG uptake in the right breast mass, which is now comparable to normal tissue (arrow). pCR was confirmed with lumpectomy.

FDG PET Imaging

FDG is the most commonly used molecular imaging agent in clinical practice for imaging tumor glycolytic metabolism with PET (Fig 6). In the most recent NCCN guidelines, FDG PET imaging can be used for optional systemic staging and restaging of patients with stage III disease, locally advanced and inflammatory breast cancer, and recurrent and/or metastatic breast cancer. It is considered most helpful when findings of standard staging studies (CT or MR imaging with bone scan) are equivocal (20).

A relatively large number of studies have been performed evaluating FDG PET for predicting pathologic response to neoadjuvant therapy (75–81). The largest prospective multicenter study involved 272 examinations in 104 patients with newly diagnosed large or locally advanced, noninflammatory primary breast cancer participating in a concurrent trial comparing two preoperative chemotherapy regimens (82). This study showed that after the first cycle of chemotherapy, a threshold of 45% decrease in SUV correctly identified 11 of 15 histopathologic responders. The negative predictive value for nonresponders was approximately 90% (34 of 38). Thus, FDG PET imaging appears to aid in predicting response to neoadjuvant chemotherapy and in identifying early nonresponders.

Results of individual studies have been evaluated in three meta-analyses (Table 4). The diagnostic performance of FDG PET for evaluating pathologic response to neoadjuvant chemotherapy in patients with breast cancer has high pooled sensitivity (range, 80%–84%) and moderate pooled specificity (range, 66%–79%) (78–80). Potential methodologic factors contributing to these values include differences in primary tumor sizes and ER status, types and sequence of chemotherapy regimens, timing of FDG PET examinations, SUV threshold values for metabolic response definition, interobserver variability of SUV measurement, and the histopathologic response criteria used (80). Small residual tumors (< 1 cm) may be false-negative due to the limited spatial resolution of whole-body PET scanners (83). Possible biologic factors include the impact of effective therapy on tumor glucose metabolism, which is the basis of using FDG PET as an early indicator of response, resulting in false-negative examinations (84) or false-positive uptake from inflammatory changes if repeat tissue biopsy is obtained for histopathologic response evaluation (78). Subgroup analysis performed by Weng et al (79) demonstrated improved accuracy when FDG PET is performed after the first or second cycle of chemotherapy and when a reduction rate cut off value of maximum SUV between 55% and 65% is used as PET criteria for response.

Thus, FDG PET imaging could potentially be used as an early in vivo test of chemosensitivity, help identify ineffective chemotherapy regimens preoperatively, and more efficiently direct patients to either alternative therapy or surgery than conventional imaging approaches. Prospective, response-guided clinical trials are needed to demonstrate that use of FDG PET data to guide neoadjuvant therapy management improves patient outcomes.

FLT PET Imaging

Tumor proliferation is a key biologic marker for therapeutic efficacy for all types of cancer treatment and may, therefore, provide a better marker of early response than glycolysis. FLT is the most commonly studied radiopharmaceutical for imaging proliferation; however, it is not yet approved by the

Table 4

Meta-Analyses of FDG PET for Evaluation of Neoadjuvant Therapy Response

Meta-Analysis	No. of Studies	No. of Patients	Pooled Sensitivity (%)	Pooled Specificity (%)	AUC	PPV (%)	NPV (%)
Cheng et al 2012 (80)	17	781	84 (80–88)	71 (67–76)	…	Not reported	Not reported
PET only	7	…	83 (74–89)	79 (72–85)	0.88	…	…
PET/CT	10	…	85 (79–90)	66 (60–72)	0.89	…	…
Wang et al 2012 (79) PET only	16	786	84 (78–88)	66 (62–70)	0.84	50 (44–55)	91 (87–94)
Mghanga et al 2013 (78) PET+PET/CT	15	745	80 (76–84)	79 (74–83)	0.88	80	80
Sheikbahaei et al 2016 (37)	10	535	71 (52–85)	77 (58–89)	Not reported	Not reported	Not reported
PET only	3	150	43 (26–63)	73 (44–91)	…	…	…
PET/CT	7	385	82 (62–92)	79 (52–93)	…	…	…

Note.—AUC = area under the curve, NPV = negative predictive value, PPV = positive predictive value. Data in parentheses are the range.

U.S. Food and Drug Administration for use outside of clinical trials (85). FLT enters cells and becomes phosphorylated by thymidine kinase-1 as part of the thymidine salvage pathway of DNA synthesis. Phosphorylated FLT cannot incorporate into DNA and becomes trapped intracellularly.

FLT uptake has been demonstrated in patients with primary and metastatic breast cancer, with a wide range of values (86,87). A small meta-analysis (n = 33 total sample size) demonstrated a significant correlation (r = 0.65) of SUV measured at FLT PET imaging with the standard clinical immunohistochemical marker of proliferation, Ki67 (88). Despite good correlation with Ki67, the signal intensity of FLT uptake is generally lower than with FDG, with potential for false-negative findings. This observation has limited the clinical utility of FLT PET/CT for staging, and further studies have focused on its potential role for predicting and monitoring therapy response.

Results of a multi-institutional phase II clinical trial (ACRIN 6688) aiming to correlate FLT uptake with pathologic response to neoadjuvant chemotherapy in 51 patients with locally advanced breast cancer were recently published (Fig 7) (89). Overall, the study found that FLT PET imaging after one cycle of chemotherapy weakly predicted pCR. This marginal predictive performance may have been due to the heterogeneous patient population and variable chemotherapy regimens included in the protocol. Thus, additional studies are needed to better define the clinical efficacy of FLT PET/CT as a test of early therapeutic response.

Imaging Amino Acid Metabolism

Amino acid transport is upregulated in many types of cancer to support the demands of increased protein synthesis and proliferation of malignant cells. A radiolabeled essential amino acid, L-methyl-^{11}C-methionine (carbon 11 [^{11}C]-methionine), has been shown to accumulate in primary and metastatic breast cancer and can be effectively imaged with PET (90). Furthermore, its uptake is associated with the fraction of cells in S phase of the cell cycle and can indirectly indicate the proliferative status of the tumor (90). There are a few small studies of ^{11}C-methionine PET imaging that suggest that early decreases in uptake as soon as 10 days after the first cycle of chemotherapy are associated with therapy response in patients with locally advanced and metastatic breast cancer (91–93). However, the logistical demands of rapid synthesis and scanning of ^{11}C-based radiopharmaceuticals, due to its 20-minute half-life, limits its use to institutions with on-site cyclotrons. Thus, recent attention has shifted toward ^{18}F-labeled amino acids.

A synthetic amino acid analog of leucine, anti-1-amino-3-^{18}F-fluorocyclobutane-1-carboxcylic acid (FACBC, fluciclovine), was recently approved by the Food and Drug Administration. While its clinical indication is for localization of biochemically recurrent prostate cancer, it may also have an application for breast cancer imaging. Higher uptake of FACBC has been demonstrated in patients with primary and metastatic breast cancer compared with normal breast tissue and benign breast lesions (94,95). Both of these studies also showed higher uptake of FACBC compared with FDG for invasive lobular carcinoma, which can be false-negative with FDG PET imaging (94,95). Ulaner et al demonstrated that changes in FACBC uptake strongly correlated with pathologic tumor response in a pilot study of 24 women with newly diagnosed, locally advanced breast cancer who underwent FACBC PET/CT before and after completion of neoadjuvant chemotherapy (Fig 8) (96). Thus, FACBC PET/CT may also be useful for evaluating response to therapy.

^{11}C-Choline PET

An alternative technique for analyzing choline metabolism in tumors with use of MR spectroscopy is to use radiolabeled choline and PET imaging. Choline is an essential component of cell membranes and also a source for lipid-based second messenger signaling molecules. After transport of choline into the cell, the enzyme choline kinase-alpha phosphorylates choline into phosphocholine, which is effectively trapped within the cells. Increased ^{11}C-choline is observed in breast malignancy compared with normal tissue (97), which reflects upregulated choline kinase-alpha

Figure 7

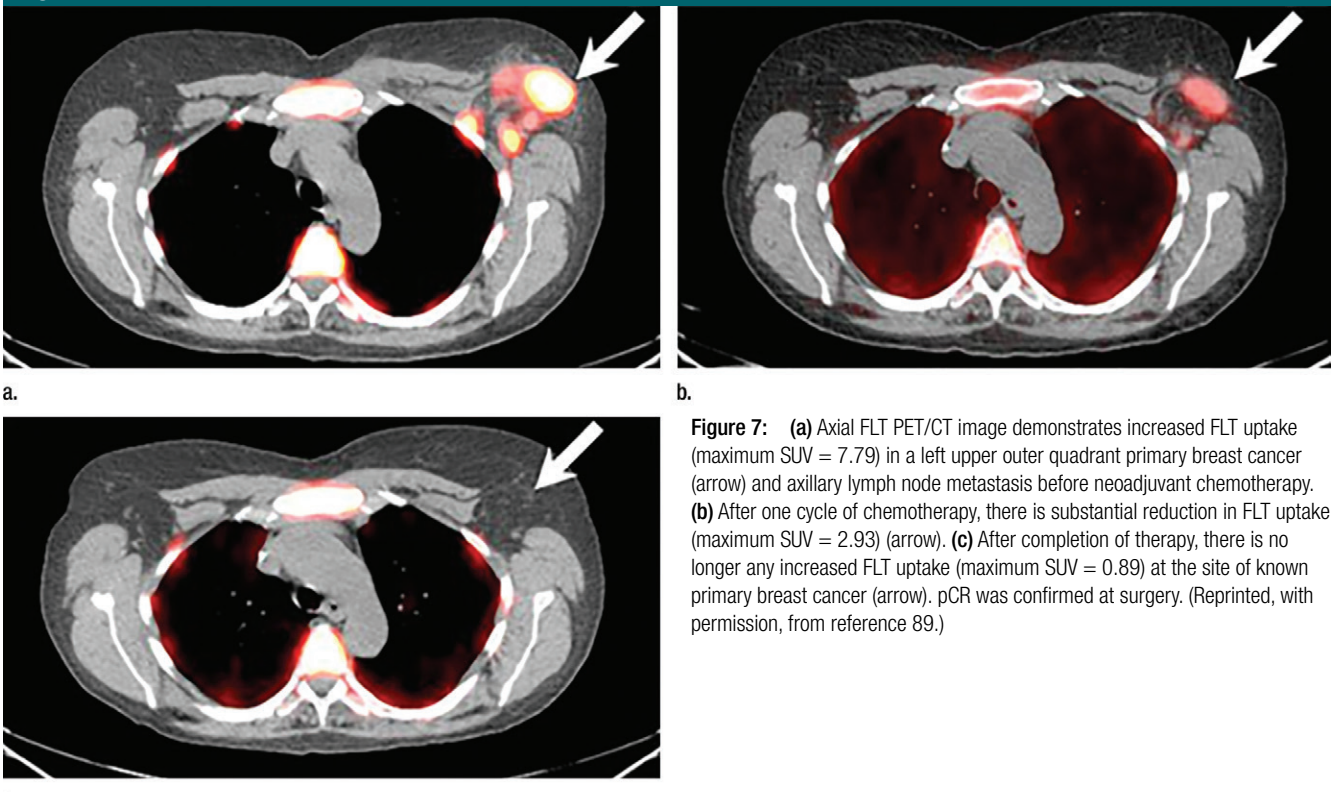

Figure 7: **(a)** Axial FLT PET/CT image demonstrates increased FLT uptake (maximum SUV = 7.79) in a left upper outer quadrant primary breast cancer (arrow) and axillary lymph node metastasis before neoadjuvant chemotherapy. **(b)** After one cycle of chemotherapy, there is substantial reduction in FLT uptake (maximum SUV = 2.93) (arrow). **(c)** After completion of therapy, there is no longer any increased FLT uptake (maximum SUV = 0.89) at the site of known primary breast cancer (arrow). pCR was confirmed at surgery. (Reprinted, with permission, from reference 89.)

expression and activity and is strongly associated with cellular proliferation (98).

^{11}C-choline PET has been used in preliminary studies of response to single-agent trastuzumab therapy in patients with HER2-positive breast cancer. Kenney et al investigated ^{11}C-choline PET imaging of 21 patients with newly diagnosed and recurrent HER2-positive, stage II to IV breast cancer (97). Six patients with eight evaluable lesions had a second scan within a month after starting trastuzumab. Among these, decreased ^{11}C-choline uptake in response to trastuzumab was identified in two patients (three lesions) who responded clinically.

Food and Drug Administration approval of this radiopharmaceutical was obtained in 2012 for men suspected of having prostate cancer recurrence. This approval, albeit for a different cancer indication, may aid in further studies of ^{11}C-choline PET for breast cancer therapy response assessment. Translational challenges that remain include its short half-life (20 minutes for ^{11}C compared with 110 minutes for ^{18}F) and limited availability due to requirement for an on-site cyclotron for radiopharmaceutical production.

PET Imaging of Tumor Blood Flow and Metabolism

An important factor in determining systemic therapy response is tumor perfusion. Tumors that are poorly perfused may not receive adequate delivery of systemic therapy to work effectively. Oxygen 15–labeled water ($H_2[^{15}O]$) can be used to image tumor blood flow, which has been shown to be increased in breast malignancies compared with normal breast tissue (99,100). Given the extremely short half-life (2 minutes) of $H_2[^{15}O]$, it can be combined with other PET imaging examinations, such as FDG, to reveal matched data regarding tumor blood flow and glucose metabolism. Mankoff et al investigated tumor blood flow and glucose metabolism in 37 patients with newly diagnosed locally advanced breast cancer prior to initiation of neoadjuvant chemotherapy. They found that a low pretreatment ratio of metabolic rate to blood flow was the best predictor of pathologic response to therapy (100). A subsequent study included comparison of blood flow and metabolism measurements before and after 2 months of neoadjuvant therapy in 35 patients with locally advanced breast cancer (101). The greatest interval changes between PET examinations were observed with $H_2[^{15}O]$ PET. Blood flow increased (+48%) in clinical nonresponders and decreased (–12%) in clinical responders. Furthermore, patients with higher blood flow after 2 months of therapy had poorer survival. Dunnwald et al (102) also showed that failure to decrease tumor blood flow from $H_2[^{15}O]$ PET or the glucose blood-to-tissue transport parameter (K1) from dynamic FDG-PET imaging was associated with higher disease recurrence and mortality in their study of 53 women with locally advanced breast cancer with imaging before and at

Figure 8

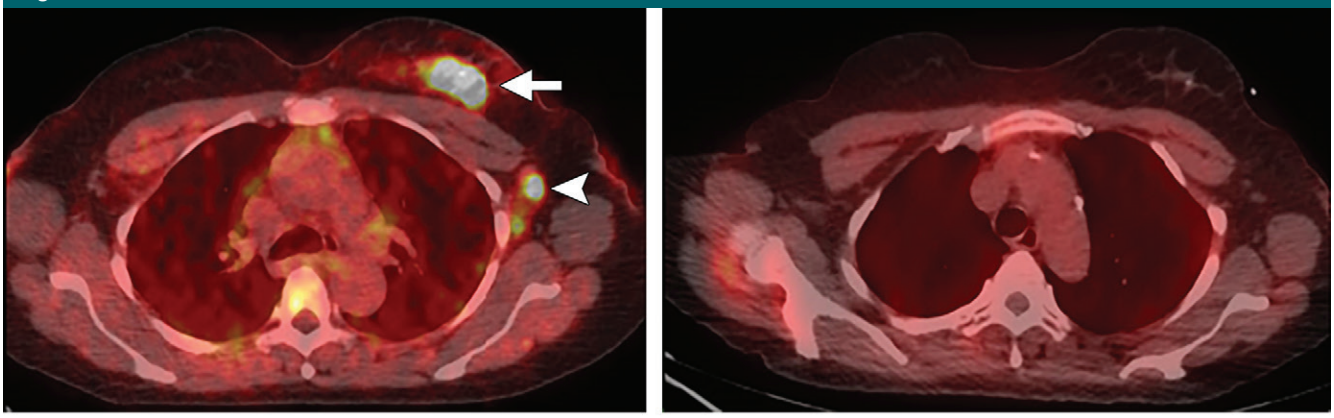

a. b.

Figure 8: Images of a 52-year-old woman with grade 2, ER-negative HER2-positive invasive ductal carcinoma. **(a)** Axial fused FACBC PET/CT image at baseline demonstrates increased uptake in the left primary breast cancer (arrow) and axillary lymph nodes (arrowhead) before neoadjuvant therapy. Following neoadjuvant therapy, FACBC avidity of all lesions decreased to background **(b)**. pCR was confirmed. (Reprinted, with permission, from reference 96.)

the midpoint of chemotherapy. Similarly, Humbert et al (103) found that persistent or elevated tumor blood flow derived from dynamic FDG PET imaging after one cycle of neoadjuvant chemotherapy was associated with lower overall survival in their study of 46 patients with triple-negative primary breast cancer. These are impactful studies showing an association between imaging response measures and overall survival.

$H_2[^{15}O]$ PET imaging can provide similar, but not identical, information as DCE MR imaging regarding changes in tumor blood flow in response to neoadjuvant chemotherapy, which is supported by studies showing a correlation between measures obtained by the two methods (104). However, given the short half-life of ^{15}O, $H_2[^{15}O]$ is not a clinically feasible method in most centers. Combining DCE MR imaging with FDG PET, or assessing blood flow from dynamic FDG PET acquisition, may be a more practical method of assessing tumor blow flow and metabolism.

Challenges and Future Directions

Standardized Reporting and Response Evaluation Criteria

There are currently no standards for reporting imaging assessment of tumor response to neoadjuvant therapy. The current edition of the American College of Radiology Breast Imaging Reporting and Data, or BI-RADS, lacks specific guidance on how to report follow-up imaging for response to therapy assessment. Typically, comparison of tumor size before and after therapy in greatest dimension measurement is reported. Descriptive patterns of tumor response may also be helpful such as mammographic lesion density decrease, change in internal echotexture, and concentric lesion shrinkage versus fragmentation with intervening normal-appearing tissue.

One approach for standardization is to utilize published tumor response criteria for evaluation of cancer therapeutics in prospective clinical trials. Response Evaluation Criteria in Solid Tumors (RECIST) version 1.1 is a commonly used method (105). The same imaging modality and method of size measurement should be used at baseline and during follow-up imaging. The types of imaging responses are categorized as complete response, partial response, stable disease, or progressive disease (Table 5). Use of RECIST 1.1 criteria for breast imaging, however, can be problematic due to lack of inclusion of mammography and recommendations against the use of US due to its subjective, operator-dependent nature. However, it does state that "MRI is the preferred modality to follow breast lesions in a neoadjuvant setting" and that "neither CT nor mammography are inadequate data to support inclusion of expanded morphologic assessments (three-dimensional tumor volumes) or functional imaging parameters as alternative assessment methods beyond tumor diameter measurement for use as clinical trial end points. One minor exception is that FDG PET can be used as confirmation for CT in determining progressive disease if new lesions are identified with this modality.

There is also no consensus on the best criteria to use for evaluating tumor response to therapy with FDG PET. Two sets have been proposed: European Organization for Research and Treatment of Cancer (EORTC) (106) and the Positron Emission Tomography Response Criteria in Solid Tumors (PERCIST), version 1.0 (107). The types of imaging responses are categorized as complete metabolic response, partial metabolic response, stable metabolic disease, or progressive metabolic disease (Table 5). The EORTC criteria were formulated from small clinical trials and they recommend that each imaging center report reproducibility measurements to ensure that the 25% cut-off point for response be greater than the institution's

Table 5

Imaging Tumor Response Evaluation Criteria

Parameter	Anatomic Imaging Response: RECIST 1.1	Functional Imaging Response: EORTC	Functional Imaging Response: PERCIST
Complete response	Complete resolution of original imaging finding	FDG uptake matches background uptake of surrounding normal tissue	FDG uptake matches background uptake of surrounding normal tissue
Progressive disease	20% increase in lesion diameter or the appearance of new lesions	SUV_{max} increase > 25% or appearance of new lesions	SUL_{peak} increase ≥ 30% or appearance of new lesions
Partial response	At least a 30% decrease in lesion diameter	SUV_{max} decrease > 25%	SUL_{peak} decrease ≥ 30%
Stable disease	Interval changes in lesion size do not qualify for partial response or progressive disease	SUV_{max} increase < 25% or SUV decrease < 25%	SUL_{peak} increase < 30% or SUL_{peak} decrease < 30%

Note.—EORTC = European Organization for Research and Treatment of Cancer, PERCIST = Positron Emission Tomography Response Criteria in Solid Tumors, RECIST = Response Evaluation Criteria in Solid Tumors, SUV_{max} = maximum SUV, SUL_{peak} = peak standardized uptake value corrected for lean body mass.

test-retest variability, which typically ranges from 10% to 20%. PERCIST criteria uses peak SUV corrected for lean body mass (SUL_{peak}) instead of maximum SUV corrected for body weight (107,108). PERCIST criteria quantifies response to therapy as a continuous variable expressed as percent change in SUL_{peak} of the most intense lesion between the baseline and posttreatment FDG PET examinations, with the interval time reported in weeks. In contrast to the EORTC criteria, PERCIST requires a change greater than 30% to distinguish partial metabolic response from progressive and stable metabolic disease. Given typical FDG PET imaging variability, changes of 30%–40% in uptake may need to be observed to ensure the most accurate assessment of tumor response (109).

It is important to keep in mind that these imaging response criteria were primarily developed for assessing metastatic disease response for all types of cancer. Additional research including correlation with patient outcomes is needed to confirm whether it is valid to apply these criteria in the neoadjuvant therapy setting for patients with primary breast cancer, which is generally more responsive to therapy compared with other cancers.

Combined Multimodality Imaging Approaches

If one could choose between MR imaging and FDG PET/CT imaging for measuring response to neoadjuvant therapy, which is more accurate? A recent meta-analysis involving 10 studies of 595 patients with breast cancer compared the diagnostic performance of MR imaging and FDG PET or PET/CT for predicting response to neoadjuvant chemotherapy (37). The analysis included studies using both PET and MR imaging in the same patient population and used postoperative histopathologic results (pCR vs nonpCR) as the reference standard. Respective pooled estimates of sensitivity and specificity were 0.88 and 0.55 for MR imaging and 0.71 and 0.77 for FDG PET or PET/CT. After excluding studies using PET imaging alone, the accuracy of FDG PET/CT (0.82 sensitivity and 0.79 specificity pooled estimates) was comparable to that of MR imaging for predicting therapy response by using summary receiver operating characteristic curve analysis. Furthermore, they found that the timing of imaging influenced diagnostic accuracy. When performed after completion of neoadjuvant therapy, MR imaging outperformed FDG PET/CT through its higher sensitivity (0.88 vs 0.57). When performed during neoadjuvant therapy, FDG PET/CT outperformed MR imaging through its higher specificity (0.69 vs 0.42). Thus, MR imaging may be better at assessing residual disease burden after therapy, while FDG PET/CT may be better at assessing response during therapy.

Simultaneous and/or integrated PET/MR imaging scanners are now commercially available for clinical use. PET/MR imaging scanners were introduced in 2010, with approximately 70 systems in place worldwide as of a 2016 report, primarily located at academic centers (110). Investigations of simultaneous breast PET/MR imaging for primary breast cancer imaging have been delayed by an initial lack of a dedicated breast radiofrequency receiver coils needed for prone positioning and high image quality. If traditional radiofrequency receiver coils are used for integrated PET/MR imaging, their presence in the field of view of the PET detectors attenuate the number of photons and can result in inaccurate SUV measurement. Thus, 16-channel breast radiofrequency coils and attention correction have been recently designed specifically for simultaneous PET/MR imaging for accurate PET quantitation and have been tested in small patient cohorts (111,112). This hybrid functional imaging modality may offer advantages for primary breast cancer therapy response assessment by combining the high sensitivity of MR imaging and high specificity of FDG PET.

Conclusion

Imaging serves several purposes when used in the neoadjuvant setting. Prior to initiation of neoadjuvant therapy, imaging should be aimed at defining the radiologic extent of disease and local-regional staging for optimal surgical planning and screening the contralateral breast. At the completion of

neoadjuvant therapy, the goal of imaging is to evaluate therapy response by determining the presence and size of residual disease and for preoperative localization planning. An emerging, yet still largely unproven, approach is imaging early during neoadjuvant therapy to identify patients who are not benefiting and direct them to alternative systemic therapy or to proceed with surgery.

The current lack of consensus practice guidelines for how best to assess tumor response to neoadjuvant therapy in breast cancer opens opportunities for research. The importance of quantitative imaging for response assessment has been recognized by major professional societies, which provide methods for improved standardization and data reproducibility to facilitate successful multicenter prospective studies. In addition to establishing diagnostic accuracy and precision data, it is important to incorporate patient outcomes as study end points to demonstrate the added value of imaging in the treatment of breast cancer patients undergoing neoadjuvant therapy. We speculate that the most accurate and clinically impactful method is a combined anatomic and functional/molecular imaging approach. The imaging modality and timing may require tailoring to the specific molecular tumor subtype and type of neoadjuvant therapy planned. We anticipate that advances in the field of radiogenomics, which links imaging phenotypes to tumor gene expression patterns (113), will help elucidate the most clinically useful imaging approach to assess neoadjuvant therapy response for breast cancer patients. Thus, an emerging paradigm of "precision imaging" is an important tool to fully realize the goal of precision medicine.

Disclosures of Conflicts of Interest: A.M.F. disclosed no relevant relationships. **D.A.M.** Activities related to the present article: disclosed no relevant relationships. Activities not related to the present article: received payment from Reflexion for board membership, consultancy fees from GE Healthcare, Blue Earth Diagnostics, grants from Siemens Healthcare, and has stock options from Reflexion. Other relationships: disclosed no relevant relationships. **B.N.J.** disclosed no relevant relationships.

References

1. Berry DA, Cronin KA, Plevritis SK, et al. Effect of screening and adjuvant therapy on mortality from breast cancer. N Engl J Med 2005;353(17):1784–1792.
2. Early Breast Cancer Trialists' Collaborative Group (EBCTCG), Davies C, Godwin J, et al. Relevance of breast cancer hormone receptors and other factors to the efficacy of adjuvant tamoxifen: patient-level meta-analysis of randomised trials. Lancet 2011;378(9793):771–784.
3. Early Breast Cancer Trialists' Collaborative Group (EBCTCG), Peto R, Davies C, et al. Comparisons between different polychemotherapy regimens for early breast cancer: meta-analyses of long-term outcome among 100,000 women in 123 randomised trials. Lancet 2012;379(9814):432–444.
4. Rastogi P, Anderson SJ, Bear HD, et al. Preoperative chemotherapy: updates of National Surgical Adjuvant Breast and Bowel Project Protocols B-18 and B-27. J Clin Oncol 2008;26(5):778–785.
5. Kaufmann M, von Minckwitz G, Mamounas EP, et al. Recommendations from an international consensus conference on the current status and future of neoadjuvant systemic therapy in primary breast cancer. Ann Surg Oncol 2012;19(5):1508–1516.
6. Gralow JR, Burstein HJ, Wood W, et al. Preoperative therapy in invasive breast cancer: pathologic assessment and systemic therapy issues in operable disease. J Clin Oncol 2008;26(5):814–819.
7. Mieog JS, van der Hage JA, van de Velde CJ. Neoadjuvant chemotherapy for operable breast cancer. Br J Surg 2007;94(10):1189–1200.
8. King TA, Morrow M. Surgical issues in patients with breast cancer receiving neoadjuvant chemotherapy. Nat Rev Clin Oncol 2015;12(6):335–343.
9. Esposito A, Criscitiello C, Curigliano G. Neoadjuvant model for testing emerging targeted therapies in breast cancer. J Natl Cancer Inst Monogr 2015;2015(51):51–55.
10. Liedtke C, Mazouni C, Hess KR, et al. Response to neoadjuvant therapy and long-term survival in patients with triple-negative breast cancer. J Clin Oncol 2008;26(8):1275–1281.
11. von Minckwitz G, Untch M, Blohmer JU, et al. Definition and impact of pathologic complete response on prognosis after neoadjuvant chemotherapy in various intrinsic breast cancer subtypes. J Clin Oncol 2012;30(15):1796–1804.
12. Cortazar P, Zhang L, Untch M, et al. Pathological complete response and long-term clinical benefit in breast cancer: the CTNeoBC pooled analysis. Lancet 2014;384(9938):164–172.
13. Houssami N, Macaskill P, von Minckwitz G, Marinovich ML, Mamounas E. Meta-analysis of the association of breast cancer subtype and pathologic complete response to neoadjuvant chemotherapy. Eur J Cancer 2012;48(18):3342–3354.
14. Petrelli F, Borgonovo K, Cabiddu M, Ghilardi M, Barni S. Neoadjuvant chemotherapy and concomitant trastuzumab in breast cancer: a pooled analysis of two randomized trials. Anticancer Drugs 2011;22(2):128–135.
15. Wuerstlein R, Harbeck N. Neoadjuvant therapy for HER2-positive breast cancer. Rev Recent Clin Trials 2017 Feb 2. [Epub ahead of print]
16. Fontein DB, Charehbili A, Nortier JW, et al. Efficacy of six month neoadjuvant endocrine therapy in postmenopausal, hormone receptor-positive breast cancer patients--a phase II trial. Eur J Cancer 2014;50(13):2190–2200.
17. Dixon JM, Renshaw L, Macaskill EJ, et al. Increase in response rate by prolonged treatment with neoadjuvant letrozole. Breast Cancer Res Treat 2009;113(1):145–151.
18. Simmons CE, Hogeveen S, Leonard R, et al. A Canadian national expert consensus on neoadjuvant therapy for breast cancer: linking practice to evidence and beyond. Curr Oncol 2015;22(Suppl 1):S43–S53.
19. Croshaw R, Shapiro-Wright H, Svensson E, Erb K, Julian T. Accuracy of clinical examination, digital mammogram, ultrasound, and MRI in determining postneoadjuvant pathologic tumor response in operable breast cancer patients. Ann Surg Oncol 2011;18(11):3160–3163.
20. National Comprehensive Cancer Network Guidelines Version 2.2016 Invasive Breast Cancer. https://www.nccn.org. Accessed December 24, 2016.
21. Helvie MA, Joynt LK, Cody RL, Pierce LJ, Adler DD, Merajver SD. Locally advanced breast carcinoma: accuracy of mammography versus clinical examination in the prediction of residual disease after chemotherapy. Radiology 1996;198(2):327–332.
22. Moskovic EC, Mansi JL, King DM, Murch CR, Smith IE. Mammography in the assessment of response to medical treatment of large primary breast cancer. Clin Radiol 1993;47(5):339–344.

23. Huber S, Wagner M, Zuna I, Medl M, Czembirek H, Delorme S. Locally advanced breast carcinoma: evaluation of mammography in the prediction of residual disease after induction chemotherapy. Anticancer Res 2000;20(1B):553–558.

24. Förnvik D, Zackrisson S, Ljungberg O, et al. Breast tomosynthesis: accuracy of tumor measurement compared with digital mammography and ultrasonography. Acta Radiol 2010;51(3):240–247.

25. Weiss A, Lee KC, Romero Y, et al. Calcifications on mammogram do not correlate with tumor size after neoadjuvant chemotherapy. Ann Surg Oncol 2014;21(10):3310–3316.

26. Li JJ, Chen C, Gu Y, et al. The role of mammographic calcification in the neoadjuvant therapy of breast cancer imaging evaluation. PLoS One 2014;9(2):e88853.

27. Adrada BE, Huo L, Lane DL, Arribas EM, Resetkova E, Yang W. Histopathologic correlation of residual mammographic microcalcifications after neoadjuvant chemotherapy for locally advanced breast cancer. Ann Surg Oncol 2015;22(4):1111–1117.

28. Chagpar AB, Middleton LP, Sahin AA, et al. Accuracy of physical examination, ultrasonography, and mammography in predicting residual pathologic tumor size in patients treated with neoadjuvant chemotherapy. Ann Surg 2006;243(2):257–264.

29. Keune JD, Jeffe DB, Schootman M, Hoffman A, Gillanders WE, Aft RL. Accuracy of ultrasonography and mammography in predicting pathologic response after neoadjuvant chemotherapy for breast cancer. Am J Surg 2010;199(4):477–484.

30. Herrada J, Iyer RB, Atkinson EN, Sneige N, Buzdar AU, Hortobagyi GN. Relative value of physical examination, mammography, and breast sonography in evaluating the size of the primary tumor and regional lymph node metastases in women receiving neoadjuvant chemotherapy for locally advanced breast carcinoma. Clin Cancer Res 1997;3(9):1565–1569.

31. Peintinger F, Kuerer HM, Anderson K, et al. Accuracy of the combination of mammography and sonography in predicting tumor response in breast cancer patients after neoadjuvant chemotherapy. Ann Surg Oncol 2006;13(11):1443–1449.

32. Mariscotti G, Houssami N, Durando M, et al. Accuracy of mammography, digital breast tomosynthesis, ultrasound and MR imaging in preoperative assessment of breast cancer. Anticancer Res 2014;34(3):1219–1225.

33. Lobbes MB, Prevos R, Smidt M, et al. The role of magnetic resonance imaging in assessing residual disease and pathologic complete response in breast cancer patients receiving neoadjuvant chemotherapy: a systematic review. Insights Imaging 2013;4(2):163–175.

34. Yuan Y, Chen XS, Liu SY, Shen KW. Accuracy of MRI in prediction of pathologic complete remission in breast cancer after preoperative therapy: a meta-analysis. AJR Am J Roentgenol 2010;195(1):260–268.

35. Wu LM, Hu JN, Gu HY, Hua J, Chen J, Xu JR. Can diffusion-weighted MR imaging and contrast-enhanced MR imaging precisely evaluate and predict pathological response to neoadjuvant chemotherapy in patients with breast cancer? Breast Cancer Res Treat 2012;135(1):17–28.

36. Marinovich ML, Houssami N, Macaskill P, et al. Meta-analysis of magnetic resonance imaging in detecting residual breast cancer after neoadjuvant therapy. J Natl Cancer Inst 2013;105(5):321–333.

37. Sheikhbahaei S, Trahan TJ, Xiao J, et al. FDG-PET/CT and MRI for evaluation of pathologic response to neoadjuvant chemotherapy in patients with breast cancer: a meta-analysis of diagnostic accuracy studies. Oncologist 2016;21(8):931–939.

38. Hylton NM, Blume JD, Bernreuter WK, et al. Locally advanced breast cancer: MR imaging for prediction of response to neoadjuvant chemotherapy—results from ACRIN 6657/I-SPY TRIAL. Radiology 2012;263(3):663–672.

39. Hylton NM, Gatsonis CA, Rosen MA, et al. Neoadjuvant chemotherapy for breast cancer: functional tumor volume by MR imaging predicts recurrence-free survival-results from the ACRIN 6657/CALGB 150007 I-SPY 1 TRIAL. Radiology 2016;279(1):44–55.

40. Mukhtar RA, Yau C, Rosen M, et al. Clinically meaningful tumor reduction rates vary by prechemotherapy MRI phenotype and tumor subtype in the I-SPY 1 TRIAL (CALGB 150007/150012; ACRIN 6657). Ann Surg Oncol 2013;20(12):3823–3830.

41. McGuire KP, Toro-Burguete J, Dang H, et al. MRI staging after neoadjuvant chemotherapy for breast cancer: does tumor biology affect accuracy? Ann Surg Oncol 2011;18(11):3149–3154.

42. Denis F, Desbiez-Bourcier AV, Chapiron C, Arbion F, Body G, Brunereau L. Contrast enhanced magnetic resonance imaging underestimates residual disease following neoadjuvant docetaxel based chemotherapy for breast cancer. Eur J Surg Oncol 2004;30(10):1069–1076.

43. Bahri S, Chen JH, Mehta RS, et al. Residual breast cancer diagnosed by MRI in patients receiving neoadjuvant chemotherapy with and without bevacizumab. Ann Surg Oncol 2009;16(6):1619–1628.

44. Wasser K, Sinn HP, Fink C, et al. Accuracy of tumor size measurement in breast cancer using MRI is influenced by histological regression induced by neoadjuvant chemotherapy. Eur Radiol 2003;13(6):1213–1223.

45. ACR Practice Parameter for the Performance of Contrast-Enhanced Magnetic Resonance Imaging (MRI) of the Breast. American College of Radiology. https://www.acr.org/~/media/2a0eb28eb59041e2825179afb72ef624.pdf. Published 2014. Accessed December 22, 2015.

46. Mann RM, Kuhl CK, Kinkel K, Boetes C. Breast MRI: guidelines from the European Society of Breast Imaging. Eur Radiol 2008;18(7):1307–1318.

47. von Minckwitz G, Blohmer JU, Costa SD, et al. Response-guided neoadjuvant chemotherapy for breast cancer. J Clin Oncol 2013;31(29):3623–3630.

48. Barker AD, Sigman CC, Kelloff GJ, Hylton NM, Berry DA, Esserman LJ. I-SPY 2: an adaptive breast cancer trial design in the setting of neoadjuvant chemotherapy. Clin Pharmacol Ther 2009;86(1):97–100.

49. Yankeelov TE, Gore JC. Dynamic contrast enhanced magnetic resonance imaging in oncology: theory, data acquisition, analysis, and examples. Curr Med Imaging Rev 2009;3(2):91–107.

50. Kuhl CK, Mielcareck P, Klaschik S, et al. Dynamic breast MR imaging: are signal intensity time course data useful for differential diagnosis of enhancing lesions? Radiology 1999;211(1):101–110.

51. Tofts PS, Brix G, Buckley DL, et al. Estimating kinetic parameters from dynamic contrast-enhanced T(1)-weighted MRI of a diffusable tracer: standardized quantities and symbols. J Magn Reson Imaging 1999;10(3):223–232.

52. Miller KD, Sweeney CJ, Sledge GW Jr. Redefining the target: chemotherapeutics as antiangiogenics. J Clin Oncol 2001;19(4):1195–1206.

53. Padhani AR, Hayes C, Assersohn L, et al. Prediction of clinicopathologic response of breast cancer to primary chemotherapy at contrast-enhanced MR imaging: initial clinical results. Radiology 2006;239(2):361–374.

54. McLaughlin R, Hylton N. MRI in breast cancer therapy monitoring. NMR Biomed 2011;24(6):712–720.

55. Marinovich ML, Sardanelli F, Ciatto S, et al. Early prediction of pathologic response to neoadjuvant therapy in breast cancer:

systematic review of the accuracy of MRI. Breast 2012;21(5):669–677.

56. Prevos R, Smidt ML, Tjan-Heijnen VC, et al. Pre-treatment differences and early response monitoring of neoadjuvant chemotherapy in breast cancer patients using magnetic resonance imaging: a systematic review. Eur Radiol 2012;22(12):2607–2616.
57. Li SP, Makris A, Beresford MJ, et al. Use of dynamic contrast-enhanced MR imaging to predict survival in patients with primary breast cancer undergoing neoadjuvant chemotherapy. Radiology 2011;260(1):68–78.
58. Woolf DK, Padhani AR, Taylor NJ, et al. Assessing response in breast cancer with dynamic contrast-enhanced magnetic resonance imaging: are signal intensity-time curves adequate? Breast Cancer Res Treat 2014;147(2):335–343.
59. DCE-MRI Technical Committee. DCE-MRI Quantification Profile, Quantitative Imaging Biomarkers Alliance. Version 1.0. Publicly Reviewed Version. QIBA, July 1, 2012. http://www.rsna.org/QIBA/. Accessed December 24, 2016.
60. Shin HJ, Kim SH, Lee HJ, et al. Tumor apparent diffusion coefficient as an imaging biomarker to predict tumor aggressiveness in patients with estrogen-receptor-positive breast cancer. NMR Biomed 2016;29(8):1070–1078.
61. Onishi N, Kanao S, Kataoka M, et al. Apparent diffusion coefficient as a potential surrogate marker for Ki-67 index in mucinous breast carcinoma. J Magn Reson Imaging 2015;41(3):610–615.
62. Partridge SC, McDonald ES. Diffusion weighted magnetic resonance imaging of the breast: protocol optimization, interpretation, and clinical applications. Magn Reson Imaging Clin N Am 2013;21(3):601–624.
63. Park SH, Moon WK, Cho N, et al. Diffusion-weighted MR imaging: pretreatment prediction of response to neoadjuvant chemotherapy in patients with breast cancer. Radiology 2010;257(1):56–63.
64. Belli P, Costantini M, Ierardi C, et al. Diffusion-weighted imaging in evaluating the response to neoadjuvant breast cancer treatment. Breast J 2011;17(6):610–619.
65. Pickles MD, Gibbs P, Lowry M, Turnbull LW. Diffusion changes precede size reduction in neoadjuvant treatment of breast cancer. Magn Reson Imaging 2006;24(7):843–847.
66. Sharma U, Danishad KK, Seenu V, Jagannathan NR. Longitudinal study of the assessment by MRI and diffusion-weighted imaging of tumor response in patients with locally advanced breast cancer undergoing neoadjuvant chemotherapy. NMR Biomed 2009;22(1):104–113.
67. Bolan PJ. Magnetic resonance spectroscopy of the breast: current status. Magn Reson Imaging Clin N Am 2013;21(3):625–639.
68. Bolan PJ, Meisamy S, Baker EH, et al. In vivo quantification of choline compounds in the breast with 1H MR spectroscopy. Magn Reson Med 2003;50(6):1134–1143.
69. Jagannathan NR, Kumar M, Seenu V, et al. Evaluation of total choline from in-vivo volume localized proton MR spectroscopy and its response to neoadjuvant chemotherapy in locally advanced breast cancer. Br J Cancer 2001;84(8):1016–1022.
70. Kvistad KA, Bakken IJ, Gribbestad IS, et al. Characterization of neoplastic and normal human breast tissues with in vivo (1) H MR spectroscopy. J Magn Reson Imaging 1999;10(2):159–164.
71. Meisamy S, Bolan PJ, Baker EH, et al. Neoadjuvant chemotherapy of locally advanced breast cancer: predicting response with in vivo (1)H MR spectroscopy—a pilot study at 4 T. Radiology 2004;233(2):424–431.
72. Baek HM, Chen JH, Nalcioglu O, Su MY. Proton MR spectroscopy for monitoring early treatment response of breast cancer to neo-adjuvant chemotherapy. Ann Oncol 2008;19(5):1022–1024.
73. Bolan PJ, Kim E, Herman BA, et al. MR spectroscopy of breast cancer for assessing early treatment response: results from the ACRIN 6657 MRS trial. J Magn Reson Imaging 2017;46(1):290–302.
74. Sardanelli F, Carbonaro LA, Montemezzi S, Cavedon C, Trimboli RM. Clinical breast MR using MRS or DWI: who is the winner? Front Oncol 2016;6:217.
75. Schelling M, Avril N, Nährig J, et al. Positron emission tomography using [(18)F] Fluorodeoxyglucose for monitoring primary chemotherapy in breast cancer. J Clin Oncol 2000;18(8):1689–1695.
76. Smith IC, Welch AE, Hutcheon AW, et al. Positron emission tomography using [(18)F]-fluorodeoxy-D-glucose to predict the pathologic response of breast cancer to primary chemotherapy. J Clin Oncol 2000;18(8):1676–1688.
77. Kim SJ, Kim SK, Lee ES, Ro J, Kang Sh. Predictive value of [18F]FDG PET for pathological response of breast cancer to neo-adjuvant chemotherapy. Ann Oncol 2004;15(9):1352–1357.
78. Mghanga FP, Lan X, Bakari KH, Li C, Zhang Y. Fluorine-18 fluorodeoxyglucose positron emission tomography-computed tomography in monitoring the response of breast cancer to neoadjuvant chemotherapy: a meta-analysis. Clin Breast Cancer 2013;13(4):271–279.
79. Wang Y, Zhang C, Liu J, Huang G. Is 18F-FDG PET accurate to predict neoadjuvant therapy response in breast cancer? a meta-analysis. Breast Cancer Res Treat 2012;131(2):357–369.
80. Cheng X, Li Y, Liu B, Xu Z, Bao L, Wang J. 18F-FDG PET/CT and PET for evaluation of pathological response to neoadjuvant chemotherapy in breast cancer: a meta-analysis. Acta Radiol 2012;53(6):615–627.
81. Wahl RL, Zasadny K, Helvie M, Hutchins GD, Weber B, Cody R. Metabolic monitoring of breast cancer chemohormonotherapy using positron emission tomography: initial evaluation. J Clin Oncol 1993;11(11):2101–2111.
82. Schwarz-Dose J, Untch M, Tiling R, et al. Monitoring primary systemic therapy of large and locally advanced breast cancer by using sequential positron emission tomography imaging with [18F]fluorodeoxyglucose. J Clin Oncol 2009;27(4):535–541.
83. Park JS, Moon WK, Lyou CY, Cho N, Kang KW, Chung JK. The assessment of breast cancer response to neoadjuvant chemotherapy: comparison of magnetic resonance imaging and 18F-fluorodeoxyglucose positron emission tomography. Acta Radiol 2011;52(1):21–28.
84. Dose-Schwarz J, Tiling R, Avril-Sassen S, et al. Assessment of residual tumour by FDG-PET: conventional imaging and clinical examination following primary chemotherapy of large and locally advanced breast cancer. Br J Cancer 2010;102(1):35–41.
85. Mankoff DA, Shields AF, Krohn KA. PET imaging of cellular proliferation. Radiol Clin North Am 2005;43(1):153–167.
86. Kenny LM, Vigushin DM, Al-Nahhas A, et al. Quantification of cellular proliferation in tumor and normal tissues of patients with breast cancer by [18F]fluorothymidine-positron emission tomography imaging: evaluation of analytical methods. Cancer Res 2005;65(21):10104–10112.
87. Smyczek-Gargya B, Fersis N, Dittmann H, et al. PET with [18F]fluorothymidine for imaging of primary breast cancer: a pilot study. Eur J Nucl Med Mol Imaging 2004;31(5):720–724.
88. Chalkidou A, Landau DB, Odell EW, Cornelius VR, O'Doherty MJ, Marsden PK. Correlation between Ki-67 immunohistochemistry and 18F-fluorothymidine uptake in patients with cancer: a systematic review and meta-analysis. Eur J Cancer 2012;48(18):3499–3513.

89. Kostakoglu L, Duan F, Idowu MO, et al. A phase II study of 3′-deoxy-3′-18F-fluorothymidine PET in the assessment of early response of breast cancer to neoadjuvant chemotherapy: results from ACRIN 6688. J Nucl Med 2015;56(11):1681–1689.

90. Leskinen-Kallio S, Någren K, Lehikoinen P, Ruotsalainen U, Joensuu H. Uptake of 11C-methionine in breast cancer studied by PET: an association with the size of S-phase fraction. Br J Cancer 1991;64(6):1121–1124.

91. Jansson T, Westlin JE, Ahlström H, Lilja A, Långström B, Bergh J. Positron emission tomography studies in patients with locally advanced and/or metastatic breast cancer: a method for early therapy evaluation? J Clin Oncol 1995;13(6):1470–1477.

92. Lindholm P, Lapela M, Någren K, Lehikoinen P, Minn H, Jyrkkiö S. Preliminary study of carbon-11 methionine PET in the evaluation of early response to therapy in advanced breast cancer. Nucl Med Commun 2009;30(1):30–36.

93. Huovinen R, Leskinen-Kallio S, Någren K, Lehikoinen P, Ruotsalainen U, Teräs M. Carbon-11-methionine and PET in evaluation of treatment response of breast cancer. Br J Cancer 1993;67(4):787–791.

94. Tade FI, Cohen MA, Styblo TM, et al. Anti-3-18F-FACBC (18F-fluciclovine) PET/CT of breast cancer: an exploratory study. J Nucl Med 2016;57(9):1357–1363.

95. Ulaner GA, Goldman DA, Gönen M, et al. Initial results of a prospective clinical trial of 18F-fluciclovine PET/CT in newly diagnosed invasive ductal and invasive lobular breast cancers. J Nucl Med 2016;57(9):1350–1356.

96. Ulaner GA, Goldman DA, Corben A, et al. Prospective clinical trial of 18F-fluciclovine PET/CT for determining the response to neoadjuvant therapy in invasive ductal and invasive lobular breast cancers. J Nucl Med 2017;58(7):1037–1042.

97. Kenny LM, Contractor KB, Hinz R, et al. Reproducibility of [11C]choline-positron emission tomography and effect of trastuzumab. Clin Cancer Res 2010;16(16):4236–4245.

98. Contractor KB, Kenny LM, Stebbing J, et al. Biological basis of [^{11}C]choline-positron emission tomography in patients with breast cancer: comparison with [^{18}F]fluorothymidine positron emission tomography. Nucl Med Commun 2011;32(11):997–1004.

99. Wilson CB, Lammertsma AA, McKenzie CG, Sikora K, Jones T. Measurements of blood flow and exchanging water space in breast tumors using positron emission tomography: a rapid and noninvasive dynamic method. Cancer Res 1992;52(6):1592–1597.

100. Mankoff DA, Dunnwald LK, Gralow JR, et al. Blood flow and metabolism in locally advanced breast cancer: relationship to response to therapy. J Nucl Med 2002;43(4):500–509.

101. Mankoff DA, Dunnwald LK, Gralow JR, et al. Changes in blood flow and metabolism in locally advanced breast cancer treated with neoadjuvant chemotherapy. J Nucl Med 2003;44(11):1806–1814.

102. Dunnwald LK, Gralow JR, Ellis GK, et al. Tumor metabolism and blood flow changes by positron emission tomography: relation to survival in patients treated with neoadjuvant chemotherapy for locally advanced breast cancer. J Clin Oncol 2008;26(27):4449–4457.

103. Humbert O, Riedinger JM, Vrigneaud JM, et al. 18F-FDG PET-derived tumor blood flow changes after 1 cycle of neoadjuvant chemotherapy predicts outcome in triple-negative breast cancer. J Nucl Med 2016;57(11):1707–1712.

104. Eby PR, Partridge SC, White SW, et al. Metabolic and vascular features of dynamic contrast-enhanced breast magnetic resonance imaging and (15)O-water positron emission tomography blood flow in breast cancer. Acad Radiol 2008;15(10):1246–1254.

105. Eisenhauer EA, Therasse P, Bogaerts J, et al. New response evaluation criteria in solid tumours: revised RECIST guideline (version 1.1). Eur J Cancer 2009;45(2):228–247.

106. Young H, Baum R, Cremerius U, et al. Measurement of clinical and subclinical tumour response using [18F]-fluorodeoxyglucose and positron emission tomography: review and 1999 EORTC recommendations. European Organization for Research and Treatment of Cancer (EORTC) PET Study Group. Eur J Cancer 1999;35(13):1773–1782.

107. Wahl RL, Jacene H, Kasamon Y, Lodge MA. From RECIST to PERCIST: evolving considerations for PET response criteria in solid tumors. J Nucl Med 2009;50(Suppl 1):122S–150S.

108. O JH, Lodge MA, Wahl RL. Practical PERCIST: a simplified guide to PET Response Criteria in Solid Tumors 1.0. Radiology 2016;280(2):576–584.

109. Harrison RL, Elston BF, Doot RK, Lewellen TK, Mankoff DA, Kinahan PE. A virtual clinical trial of FDG-PET imaging of breast cancer: effect of variability on response assessment. Transl Oncol 2014;7(1):138–146.

110. Spick C, Herrmann K, Czernin J. 18F-FDG PET/CT and PET/MRI perform equally well in cancer: evidence from studies on more than 2,300 patients. J Nucl Med 2016;57(3):420–430.

111. Oehmigen M, Lindemann ME, Lanz T, Kinner S, Quick HH. Integrated PET/MR breast cancer imaging: attenuation correction and implementation of a 16-channel RF coil. Med Phys 2016;43(8):4808.

112. Dregely I, Lanz T, Metz S, et al. A 16-channel MR coil for simultaneous PET/MR imaging in breast cancer. Eur Radiol 2015;25(4):1154–1161.

113. Rutman AM, Kuo MD. Radiogenomics: creating a link between molecular diagnostics and diagnostic imaging. Eur J Radiol 2009;70(2):232–241.